

# MR Imaging of Compact White Matter Pathways

John T. Curnes<sup>1</sup>  
 Peter C. Burger<sup>2</sup>  
 William T. Djang<sup>1</sup>  
 Orest B. Boyko<sup>1</sup>

A prominent decreased signal intensity can be seen in many of the heavily myelinated, compact fiber pathways of the brain on T2-weighted spin-echo MR images (TR = 2500 msec, TE = 80 msec). These areas include the anterior commissure, internal capsule, optic tract and radiations, fornix, mammillothalamic tract, superior frontooccipital fasciculus, cingulum, corpus callosum, uncinate fasciculus, and superior longitudinal fasciculus. All these pathways could be identified in normal subjects 3 years old and older when 1.5-T axial and coronal images of 50 adults and 17 children were reviewed. Correlation of the in vivo and postmortem MR appearance of two human brains with Perls and Luxol fast blue stains indicates that the short T2 reflects heavy myelination and fiber density, not iron deposition. This is in contrast to the short T2 signal seen in the subcortical U fibers and deep nuclei of the brain that result from iron deposition. These pathways also differ from areas of brain iron accumulation in that (1) they may appear as areas of short T1 on partial-saturation or inversion-recovery pulse sequences and (2) they can be seen with regularity in all patients over 3 years of age. It is important to distinguish between the effect of the myelin sheath and the effect of brain iron on the T2 relaxation values seen in the normal brain since both result in shortened T2 relaxation.

The importance of the role of these fiber tracts in disease processes and in modifying the spread of vasogenic edema and tumor needs further investigation.

The CT appearance of fiber pathways of the brain and how these structures can modify the spread of cerebral edema was initially described by Cowley [1]. MR imaging provides an even more sophisticated display of cerebral white matter, based partly on differences in water content, with improved contrast resolution of structures that cannot be appreciated on CT scanning.

Iron deposition in the deep nuclei of the brain and subcortical U fibers has been shown recently to modify the signal of water molecules in those regions, resulting in a shortened T2 relaxation [2–4]. Examining several other areas of decreased signal intensity in the brain that correspond to white matter tracts or commissures, one might ask if brain iron deposition in these pathways, as in the subcortical U fibers, accounts for their characteristic decreased T2 relaxation time on spin-echo images. We attempted to define the anatomic features underlying this MR appearance, and to determine if the low signal intensity was correlated with myelination, stainable iron deposition, or both.

## Materials and Methods

All studies were performed on a superconducting magnet operating at 1.5 T.\* At least two standard pulse sequences were used: (1) A multislice, multiecho pulse sequence, 2500/40,80 (TR/first-echo TE, second-echo TE), to obtain T2-weighted information and (2) a multislice spin-echo partial-saturation pulse sequence, 500/20 (TR/TE), to obtain T1-weighted information. A slice thickness of 5 mm was used with a 128 × 256 matrix. All images were obtained with two signal averages.

The scans of 50 normal adults 16–67 years old were analyzed by one of us for the presence and appearance of the following tracts: anterior commissure, optic tract, internal

Received February 17, 1988; accepted after revision June 13, 1988.

<sup>1</sup> Department of Radiology, Box 3808, Duke University Medical Center, Durham, NC 27710. Address reprint requests to J. T. Curnes.

<sup>2</sup> Department of Pathology, Duke University Medical Center, Durham, NC 27710.

*AJNR* 9:1061–1068, November/December 1988

0195–6108/88/0906–1061

© American Society of Neuroradiology

\* General Electric, Milwaukee, WI.



capsule, optic radiations and inferior frontooccipital fasciculus, cingulum, superior frontooccipital fasciculus, internal capsule, mammillothalamic tract, fornix, brachium pontis, corpus callosum, uncinate fasciculus, and superior longitudinal fasciculus. In addition, 17 normal studies from the pediatric population, ages 1–13 years, were examined to determine the relative time of appearance of these fiber tracts.

The MR appearance was correlated with stains for ferric iron and myelin in two postmortem brain specimens obtained from patients 1 and 29 years old. The formalin-fixed brains were first imaged with 2500/80/1 (TR/TE/excitations) and a  $256 \times 256$  matrix. To determine the topographic distribution of ferric ( $\text{Fe}^{3+}$ ) iron in the brain, one brain was sectioned in the horizontal plane and the other in the coronal plane; both were washed overnight in deionized water, immersed in a modified Perls solution for 20 min, and rinsed in deionized water. The Perls staining results in concentration-related blue intensity in areas of brain with ferritin and other ferric compounds [2]. Finally, corresponding paraffin-embedded whole-brain sections were stained with H and E/Luxol fast blue, with areas of myelin staining deep blue.

Additional anatomic relationships were determined from an atlas of myelin-stained human brain sections [5].

## Results

### *Image Analysis*

The anterior commissure, optic radiation, inferior frontooccipital fasciculus, cingulum, superior frontooccipital fasciculus, internal capsule, mammillothalamic tract, fornix, brachium pontis, corpus callosum, uncinate fasciculus, and superior longitudinal fasciculus could be consistently identified in vivo in each adult patient on axial- and coronal-plane heavily T2-weighted spin-echo images, 2500/80. These structures appeared as areas of decreased intensity as compared with the gray matter as well as with surrounding white matter. On T1-weighted images, only the anterior commissure, corpus callosum, internal capsule, and fornix could be identified, appearing as tracts of increased signal intensity. T1-weighted images provided insufficient contrast between the other fiber pathways and the surrounding white and/or gray matter.

Of the 17 pediatric patients, the structures were identified in all nine children 3–13 years old. In two 2-year-old patients, the mammillothalamic tract, fornix, and superior longitudinal fasciculus could not be delineated definitively. In four 1-year-old patients, the corpus callosum, internal capsule, brachium pontis, and optic radiation were the major visible tracts (Figs. 1A–1E). Foci of decreased signal intensity in deep nuclei of the brain were not observed in any of the 11 patients aged 3 years old and younger.

In the two specimens, decreased signal intensity of the white matter tracts seen on postmortem MR were identical to those seen on in vivo images, and correlated with myelin staining but not with iron staining. No iron was detected in the 1-year-old patient, yet myelination of internal capsule, corpus callosum, and optic radiation was well demonstrated on images and histologic section (Figs. 1A–1E). In the 29-year-old, areas of iron deposition in deep nuclei contrasted with an absence of Perls-related staining in white matter fiber pathways, except subcortical U fibers (Fig. 2C). Very slight staining was observed in the centrum semiovale. Luxol fast blue staining for myelin (Fig. 2D) confirmed that the decreased

T2 on in vivo and postmortem MR corresponded to myelination.

## Discussion

Our study indicates that the decreased signal intensity of the major white-matter pathways on MR imaging reflects myelination, as opposed to iron deposition. First, the decreased signal intensity secondary to iron deposition is confined specifically to the deep nuclei and subcortical U fibers [2–4]. The decreased signal intensity in most white matter pathways seen on T2-weighted images correlates precisely with heavily myelinated fiber bundles, as demonstrated with myelin stains and anatomic atlas correlation [5]. The finding of iron deposits in the subcortical U fibers is enigmatic, and may reflect unique enzymes or selective deposition of metabolic by-products of aging [2]. Second, some pathways also exhibit a short T1 on T1-weighted images, in contrast to ferritin in the brain, which does not affect the longitudinal relaxation (T1) [2]. The relative contribution of lipid vs protein vs water content to this increased signal on T1 images remains controversial. The short T1 is best appreciated, however, in the larger, most heavily myelinated pathways, suggesting that myelin lipids play some role in altering T1 relaxation. Finally, identification of white matter fiber tracts on MR is consistently seen in the pediatric age group, whereas iron deposition is age-related and most consistently demonstrated after the second decade of life [2].

### *Myelination*

Lemire et al. [6], Yakovlev and Lecours [7], and Brody et al. [8] studied the cycles of myelination in fetal and postnatal material, finding that myelination was in most pathways complete between ages 1 and 2, depending on the specific fiber tract. They noted that myelination in some pathways, such as the intracortical association areas, proceeds into the second or third decade of life. Therefore, myelination does not terminate at the end of the first postnatal year but continues, particularly in the hemispheric white matter, into early adulthood.

Several authors have documented the changes on MR corresponding to myelination of the white matter in the developing neonate and infant [9–12]. Myelination of the white matter has been shown to result in a decreased T1 and T2 relaxation. Incompletely myelinated neurons have less lipid content but more free water content than do fully myelinated fibers.

Holland et al. [9] found that the sharp decrease in both T1 and T2 values seen in the white matter was most pronounced in the first year of life. They attributed this progressive decline in relaxation times to the increase in myelination with subsequent decrease in water content and found that this correlates with reported autopsy studies in infants.

Our MR and pathologic findings corroborate the work of these authors, and a relatively normal adult appearance can be seen at age 2, with identification of all major fiber tracts by age 3 (Fig. 1).



On the basis of high-resolution spectra, it is said that the lipid content is of less significance than the water content in determining white/gray differentiation on MR [9]. However, relative lipid concentration (specifically myelin) seems to play

a central role in determining contrast between discrete areas of the white matter interspersed among other fiber tracts. When our images are correlated with myelin-stained sections at the same level, as well as referenced to established atlases

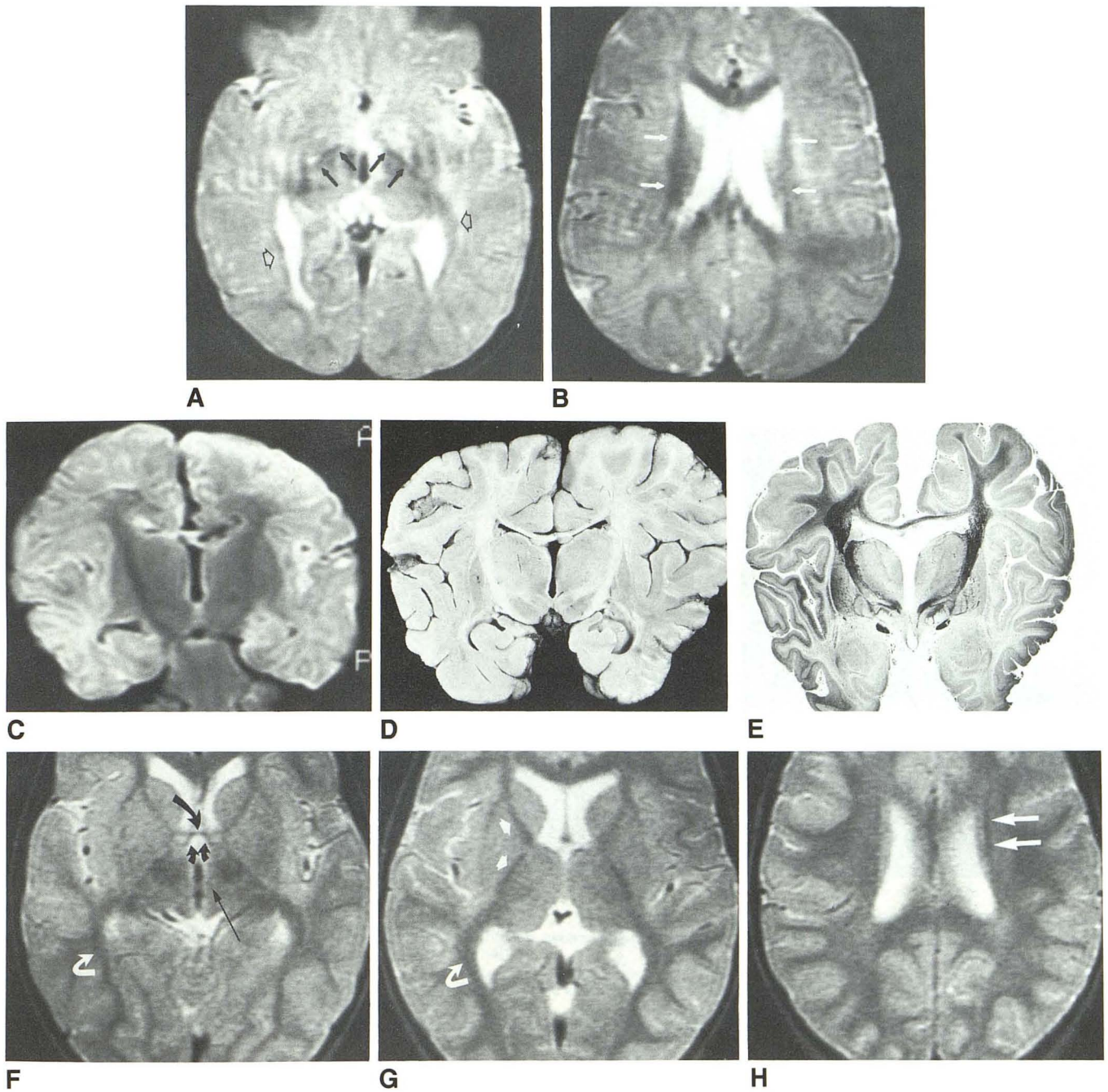


**Fig. 1.—Age-related changes in myelination.**  
**A and B,** T2-weighted images of 1-year-old boy.  
**A,** Note posterior limb of internal capsule (solid arrows) and optic radiation (open arrows). Flow artifact from CSF in third ventricle is present.  
**B,** Converging fibers of internal capsule (arrows), as well as forceps major and minor of corpus callosum, appear dark.  
**C–E,** Coronal views of postmortem specimen from a different 1-year-old boy.  
**C,** MR image at level of posterior limb correlates well with areas of decreased T2 seen on in vivo axial images representing internal capsule fibers. Corpus callosum is obscured by formalin pooled in interhemispheric fissure.  
**D,** Perl's stain is negative, as expected for iron at this age.  
**E,** Myelin preparation highlights internal capsule, optic tracts, and corpus callosum as dark areas of stain uptake.  
**F–H,** Axial T2-weighted images in 3-year-old. Note adult appearance, with excellent delineation of fiber tracts. Anterior commissure (long curved black arrow), fornix (short curved black arrows), mammillothalamic tract (long straight black arrow), internal capsule (short straight white arrows), optic radiation (curved white arrows), and superior frontooccipital fasciculus (long straight white arrows).



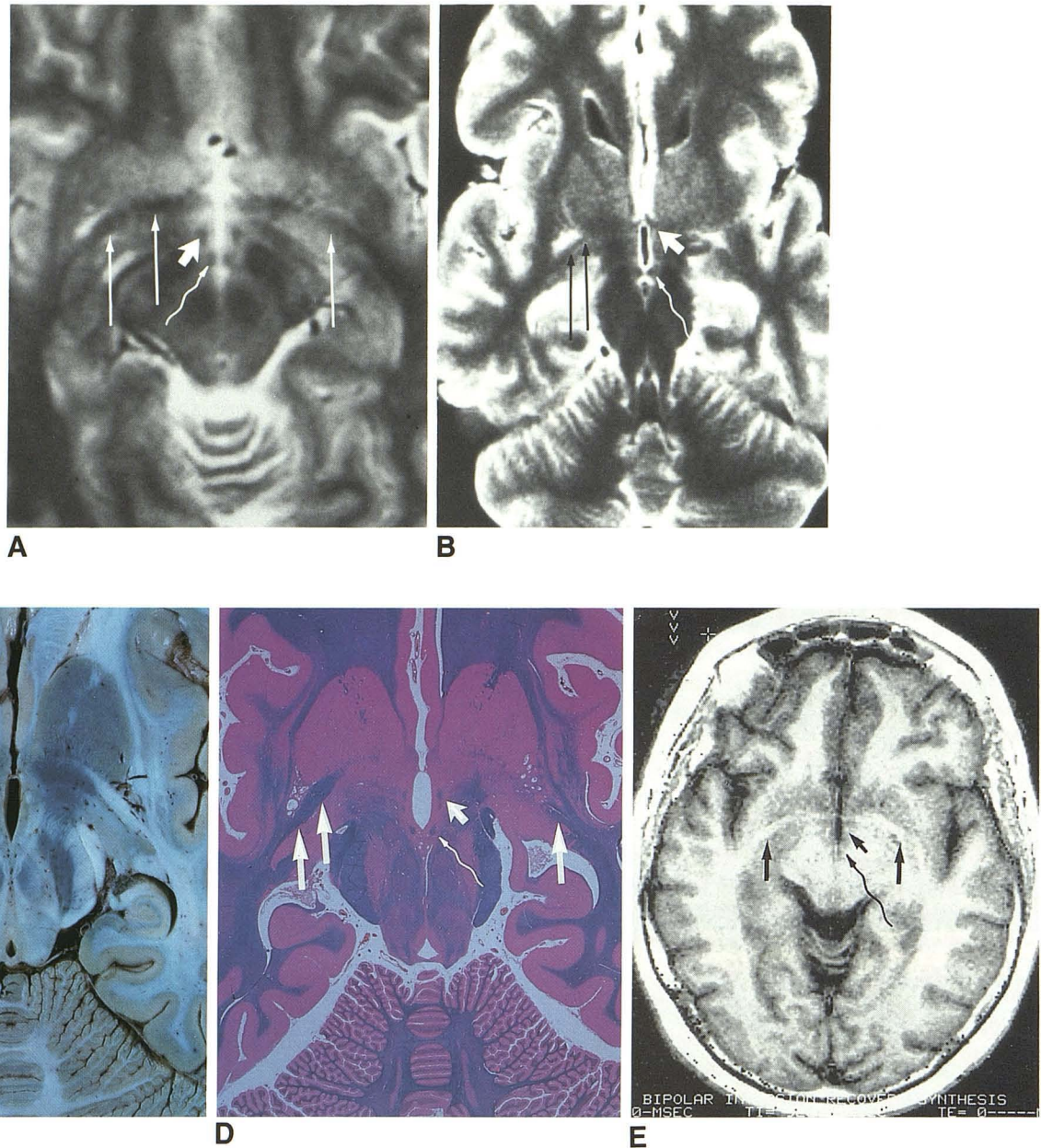


**Fig. 2.—Hypothalamic area.**  
**A,** Axial T2-weighted image, 2500/80, in normal 30-year-old woman shows anterior commissure (*long straight arrows*), fornix (*short straight arrow*), and mammillothalamic tract (*wavy arrow*).  
**B–E,** Sections from postmortem specimen of 29-year-old women.  
**B,** T2-weighted image. Decreased T2 areas correspond with those areas on in vivo scan (**A**). Anterior commissure (*black arrows*), fornix (*straight white arrow*), and mammillothalamic tract (*wavy arrow*).  
**C,** Perls stain shows that these tracts are devoid of ferritin or similar ferric iron products. Note uptake of stain in red nuclei, substantia nigra, globus pallidus, and putamen.  
**D,** Myelin preparation correlates well with in vivo T2-weighted image (**A**) and postmortem MR image (**B**), highlighting major fiber tracts with intense blue uptake of stain. Note that fornix (*short straight arrow*) and mammillothalamic tract (*wavy arrow*) have given off smaller fiber bundles, not seen on MR, whose destination is the hypothalamus. Note anterior commissure (*long straight arrows*) merging with external and extreme capsules.  
**E,** Inversion-recovery synthesis image, 3020–920/0 (TR/T1/TE). Only anterior commissure (*long straight arrows*), fornix (*short straight arrow*), and mammillothalamic tract (*wavy arrow*) are clearly seen.

of the brain based on myelin-stained material [5], a clear distinction between these discrete fiber bundles and the rest of the brain can be appreciated. Barkovich et al. [12] have shown that T1 images are most useful in the first 6 months of life, primarily because of lipid's effect on T1 relaxation.

After this age, T2-weighted images are more useful because changes related to water density in white matter predominate.

One of us has confirmed the dependence of magnetic field strength on visualization of structures containing brain iron, as was described by Drayer et al. [2], with poor discrimination



of red nuclei, substantia nigra, and globus pallidus on images obtained at 0.5 vs 1.5 T [13]. However, the large supratentorial white matter fiber tracts such as the cingulum, corpus callosum, and superior frontooccipital fasciculus were seen in over 75% of normal patients at 0.5 T [13], reflecting and emphasizing the different behavior of lipid vs iron in modifying the local environment of water molecules.

#### Fiber Density in Myelinated Tracts

In an effort to determine those factors that contribute to the MR appearance of compact fiber bundles, we referred to studies in humans and animals addressing the total number of fibers, as well as the percentage of myelinated fibers, in several of the large tracts of the brain [14, 15]. These results are summarized in Table 1. No quantitative numbers could be found for the cingulum, optic radiation, uncinete fasciculus, or superior frontooccipital fasciculus.

The density of fibers in the spinal cord and cerebral peduncle is 60,000–90,000/mm<sup>2</sup> [15]. Because the pyramidal tract begins as the fan-shaped corona radiata of the supratentorial white matter, one may extrapolate a density of much less than 60,000–90,000 fibers/mm<sup>2</sup> in the supratentorial white matter. This can be confirmed by the relative intensity of myelin staining of the corona radiata as displayed in the atlas of Riley (Fig. 3D) [5] vs other pathways and explains why compact fiber bundles stand out as discrete structures on MR.

#### Specific Fiber Pathways

**Internal capsule.**—As seen in the axial plane, the internal capsule is customarily divided into three zones. The anterior limb consists of thalamocortical and corticopontine radiations. The genu transmits primarily the corticobulbar fibers. Finally, the posterior limb carries corticospinal tracts and superior thalamic radiations, with geniculocalcarine fibers traversing the most posterior aspect.

On axial T2-weighted images, the anterior limb of the internal capsule is well defined (Fig. 3F), whereas the genu and posterior limb are inseparable from the medial portion of the globus pallidus, reflecting an equal effect of iron (globus pallidus) vs myelin (capsule) on T2 relaxation in the adult. In children, the posterior limb of the internal capsule is visualized as a separate structure since myelination is nearly complete before iron deposition begins (Figs. 1A and 1G). Also, the internal capsule is discrete on T1-weighted images due to the

disparity between the influence of ferritin on T1 relaxation (none) and myelin or fat (shortens T1) (Fig. 2E).

A slightly increased intensity on T2 images at the level of the optic radiation and retrolenticular internal capsule on horizontal sections at the level of the anterior commissure (Fig. 3F) is attributed to a lack of iron [2]. However, myelin-stained sections from our work (Fig. 2D) and that of others [5] suggest that the myelin density is lower in this area (corticospinal fibers) as compared with the more anterior corticopontine and corticofugal fibers, also present in the posterior limb. We suggest that the decreased density of corticospinal fibers relative to the rest of the posterior limb, in addition to lack of ferritin, best explains the observed appearance on MR.

**Mammillothalamic tract.**—The mammillothalamic tract is an efferent tract from the mammillary body, medial nucleus. It ascends through the hypothalamus adjacent to the third ventricular wall, traverses the medial thalamic nucleus, and ends in the anterior thalamic nucleus. It is said that this fasciculus is a part of a descending olfactory system.

This tract is seen particularly well because it is surrounded by hyperintense CSF medially, and less hyperintense hypothalamic nuclei laterally (Fig. 2). It is visible only on one or two cuts before it ends in the anterior thalamic nucleus. The other bundle of mammillary efferent fibers, the mammillotegmental tract, cannot be identified consistently on axial or coronal images.

**Fornix.**—The fornix is the main efferent system of the hippocampal formation. It begins as the alveus, converges to form the fimbria, terminates in the lateral mammillary nucleus, and contains many fibers that connect cortical neurons to deep nuclei. It consists of several sections, including the columns, body, commissure, and posterior crus.

The anterior portion of the columns and the body are easily identified on MR images, and are particularly well contrasted against the bright CSF on T2-weighted images (Fig. 1). Like the mammillothalamic tract, the most proximal anterior portion of the fornix can be seen as two small dots bounded medially by the third ventricle and laterally by the hypothalamus. As the columns of the fornix arch superiorly, the body and commissure occasionally can be seen as areas of decreased T2 similar in intensity to, but just below, the corpus callosum. The fimbria of the fornix can be seen as it enters the hippocampal formation, just lateral to the pulvinar (Fig. 3F).

**Anterior commissure.**—A primitive commissural system of the brain, the anterior commissure connects the hippocampal gyri, the amygdala, and other parts of the temporal lobe. Its precise function remains enigmatic. The phenomenon of "mirror foci" in seizures of unilateral temporal lobe lesions is probably mediated through this tract.

Naidich et al. [16] first brought our attention to the anterior commissure as a landmark with superb anatomic-MR correlation. The anterior commissure is seen quite well on T1-weighted images (500/20) or on intermediate-weighted spin-echo images (2500/40) because of its contrast with the tissues surrounding it. Naidich et al. also demonstrated that it can be seen well on sagittal T1-weighted images as an area of increased intensity reflecting its heavy myelination. Because of its myelination, its identification is even more apparent on heavily T2-weighted images (2500/80) (Figs. 1F, 2,

**TABLE 1: Density of Fibers in Various Fiber Tracts [14, 15]**

Structure	Fibers/mm <sup>2</sup>
Corpus callosum	340,000
Anterior commissure	800,000
Fornix	200,000
Mammillothalamic tract	150,000
Optic nerve	500,000
Cerebral peduncle and spinal cord	75,000



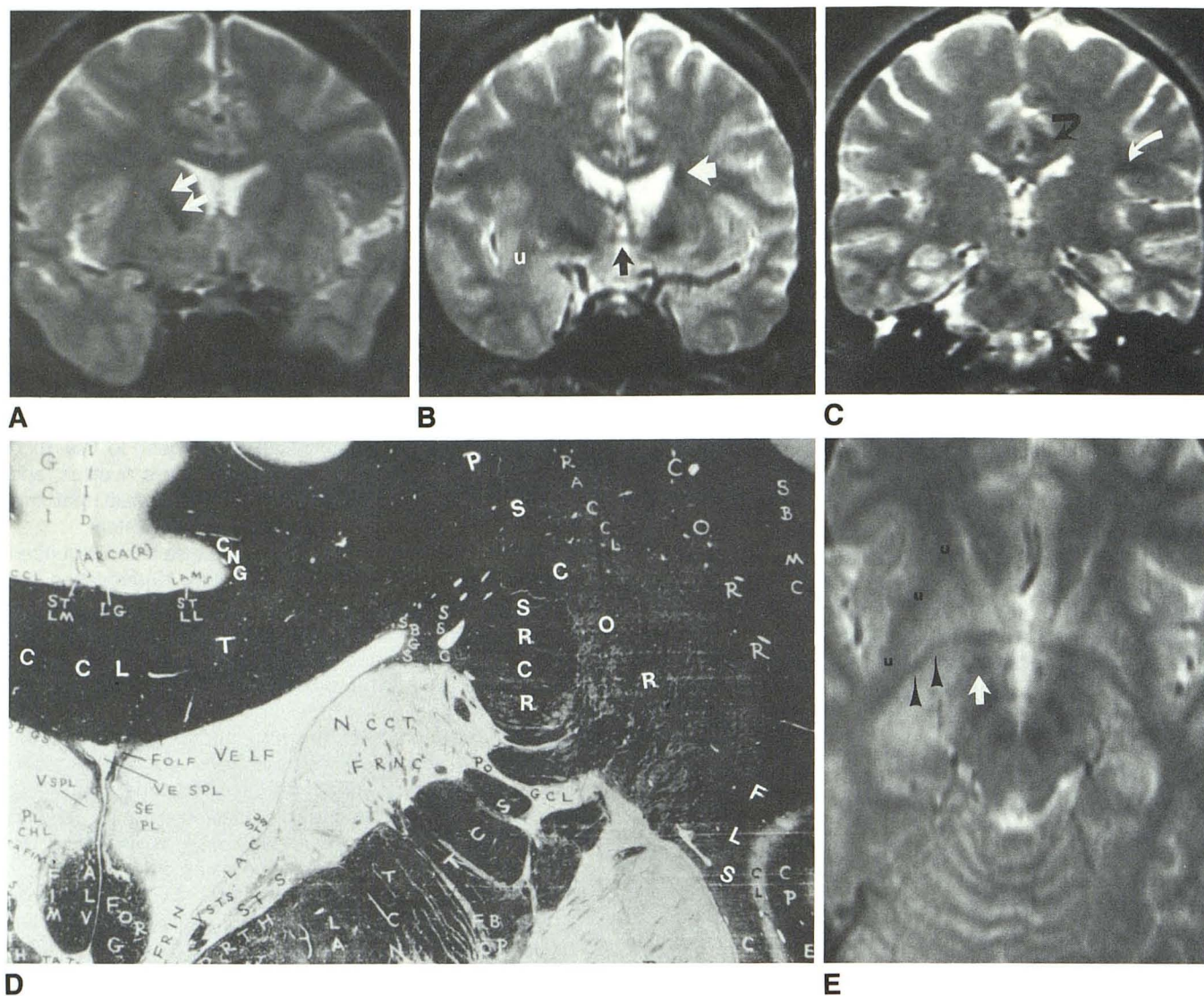


Fig. 3 legend is on opposite page.

3B, and 3D). As also shown by Naidich et al., the posterior crus of the anterior commissure can be identified consistently on MR images. This posterior crus can be followed laterally through the globus pallidus, where it merges with the white matter of the uncinete fasciculus (Fig. 3E).

*Superior frontooccipital fasciculus.*—This large bundle of fibers lies between the corpus callosum and the radiation of the internal capsule. The bundle is more compact in the frontal region, becoming less distinct as it courses toward the occipital lobe. The corpus callosum contributes heavily to this bundle, which also carries thalamocortical radiations.

Best seen on coronal images at the level of the foramen of Monro, it appears as a dark rounded bundle just lateral to the corner of the lateral ventricle and measures about 5 mm in diameter in the adult (Figs. 1H, 3B, and 3D). Axial images reveal a long straight fasciculus paralleling the cingulum, within the substance of the centrum semiovale (Fig. 3G). We disagree with Atlas et al. [17], who labeled this structure the

lateral longitudinal striae, a fiber tract lying *medial*, not lateral, to the body of the lateral ventricle.

*Cingulum.*—The cingulum is an association bundle contained within the cingulate gyrus just dorsal to the corpus callosum. The cingulum occupies a central position within the limbic system. Its function is poorly understood but appears to be integral in coordinating the brain's response to various emotional behaviors.

It is well seen on coronal T2-weighted MR images throughout its front-to-back course, just deep to the cingulate gyrus (Figs. 3C and 3D). On axial images, it can be found as a medial longitudinal structure roughly paralleling the superior frontooccipital fasciculus (Fig. 3H). We disagree again with Atlas et al. [17], who labeled this structure the medial longitudinal striae, which lies *below* the cingulate gyrus.

*Optic radiation.*—These fibers, originating in the lateral geniculate body, traverse the retrolenticular portion of the internal capsule and form the Meyer loop (Fig. 4). It, along



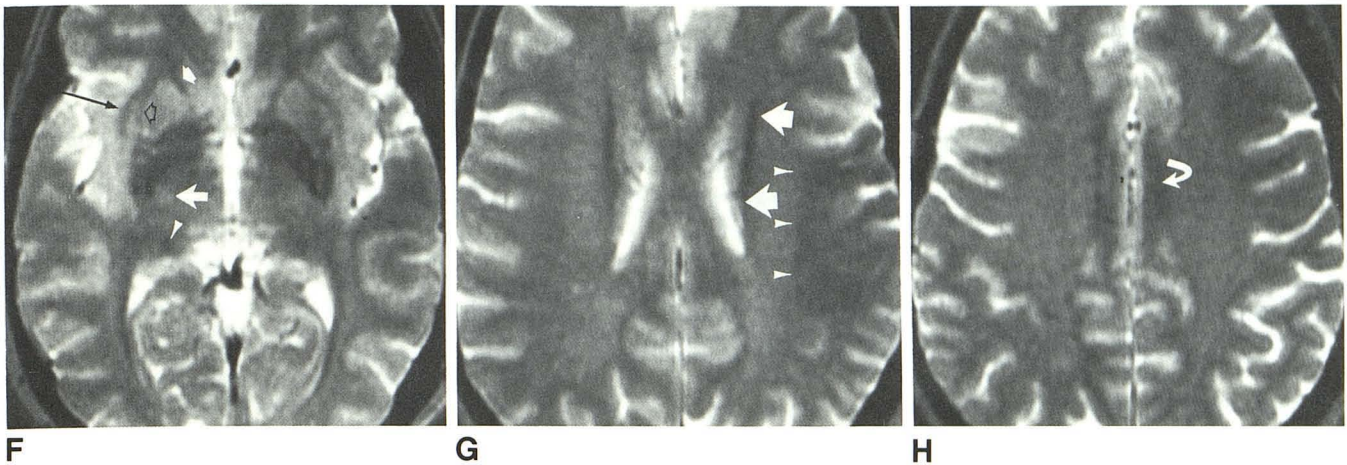


Fig. 3.—Capsules and longitudinal tracts.

- A, Coronal T2-weighted image. Internal capsule (arrows) is intersected by strands representing rostroventral contiguity of caudate and putamen.
- B, Superior frontooccipital fasciculus (white arrow) is most prominent anteriorly at this level, becoming less well defined posteriorly (C). Uncinate fasciculus (u) is seen, as well as anterior commissure (black arrow).
- C, Superior longitudinal fasciculus (white arrow) and cingulum (black arrow) are well visualized on this coronal section.
- D, Coronal myelin-stained section of human brain. Pertinent structures include body of corpus callosum (CCLT), cingulum (CNG), superior frontooccipital fasciculus (SRCR), superior longitudinal fasciculus (FLS), and corona radiata (PSCOR). (Reprinted from [5], with permission.)
- E, Uncinate fasciculus (u) interconnects frontal and temporal lobes, merging with anterior commissure fibers (arrowheads). Section of optic tract is seen at same level (arrow).
- F, External capsule (open arrow) and extreme capsule (solid black arrow) merge anteriorly with uncinate fasciculus and anterior limb of internal capsule (small white arrow). Fimbria of fornix is also identified (arrowhead). Note relatively increased signal marking corticospinal tract within posterior limb (large white arrow).
- G, Superior frontooccipital fasciculus (arrows) displays a more dense, compact appearance anteriorly. Superior longitudinal fasciculus is less well defined (arrowheads).
- H, Cingulum (arrow) is present on next axial section superior to corpus callosum.

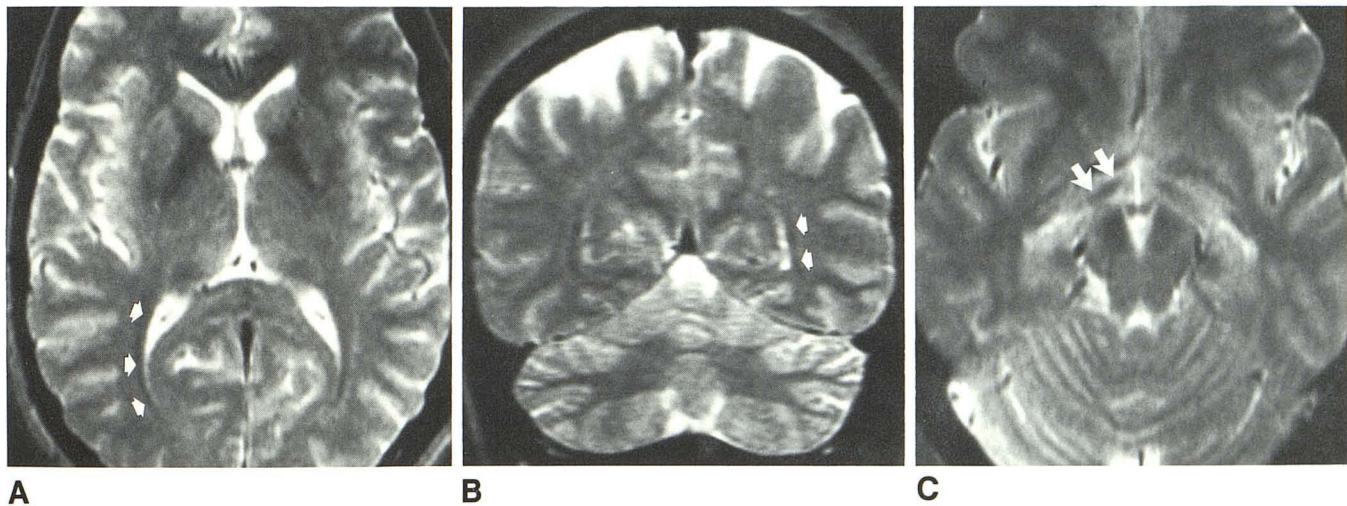


Fig. 4.—Optic pathways.

- A and B, Axial (A) and coronal (B) T2-weighted images depict long thin geniculocalcarine pathway as it curves around occipital horn (arrows).
- C, Axial T2-weighted image at level of mammillary bodies reveals midportion of optic tracts bilaterally (arrows).

with the inferior longitudinal fasciculus, can be seen as a dark band on T2-weighted images just lateral to the occipital horn and tapetum.

*Brachium pontis or middle cerebellar peduncle.*—These fibers originate in the pontine nuclei and enter the substance of the cerebellum. It is one of the earliest tracts visualized on MR, seen on both T1 and T2 images by 6 months of age

[9]. It is difficult to distinguish this mass of fibers from the inferior and superior cerebellar peduncles.

It is heavily myelinated, as demonstrated on myelin-stained and T2-weighted images, and well contrasted between the fourth ventricle medially and gray matter peripherally.

*Uncinate fasciculus.*—This important bundle can be seen to course through the lower part of the external capsule,



interconnecting the frontal and temporal lobes. It allows the spread of edema and tumor from one location to another, permitting false frontotemporal clinical localizing signs and rapid remote spread of glioma [1].

More difficult to identify on axial than on coronal images, the uncinate fasciculus can be seen as a dark area below the claustrum whose fibers merge imperceptibly with the external and extreme capsule (Fig. 3E). It is also intimately associated with the diverging fibers of the anterior commissure as they spread through the temporal lobe (Figs. 3B and 3D).

*Superior longitudinal fasciculus.*—This group of superiorly located fibers is loosely associated with the arcuate fasciculus posteriorly. A large irregular mass, its fibers merge with parts of the parietal and occipital lobes posteriorly. It can be seen lateral to the superior frontooccipital fasciculus, just above the insula (Figs. 3C, 3D, and 3G).

### Summary

Correlation of anatomic atlases, Perls and myelin stains, and data regarding normal myelination in the developing infant shows that the short T2 of fiber tracts other than the subcortical U fibers on MR is related to the development and density of myelinated axons rather than the deposition of stainable iron. The relative involvement of these tracts in demyelination diseases, ischemia, or dysmyelinating processes is currently unknown but is the subject of ongoing investigation, as is the role of these fiber tracts in modifying the spread of vasogenic edema and tumor.

### REFERENCES

- Cowley AR. Influence of fiber tracts on the CT appearance of cerebral edema: anatomic-pathologic correlation. *AJNR* 1983;4:915-925
- Drayer BP, Burger P, Darwin R, et al. Magnetic resonance imaging of brain iron. *AJNR* 1986;7:373-380
- Drayer BP, Johnson PC, Hodak JA, Flom R, Byrd R. MR images of the arcuate (subcortical "U") fibers. Presented at the annual meeting of the American Society of Neuroradiology, New York City, 1987
- Rutledge JN, Hilal SK, Silver AJ, et al. Study of movement disorders and brain iron by MR. *AJNR* 1987;8:397-411
- Riley HA. *An atlas of the basal ganglia, brainstem, and spinal cord*. Baltimore: Williams & Wilkins, 1943
- Lemire RJ, Loeser JD, Leech RW, Alvord EC. Normal and abnormal development of the human nervous system. Hagerstown, MD: Harper & Row, 1975
- Yakovlev PI, Lecours AR. The myelographic cycles of regional maturation of the brain. In: Urinowski A, ed. *Regional development of the brain in early life*. Oxford: Blackwell, 1964:3-70
- Brody BA, Kinney HC, Kloman AS, Gilles FH. Sequence of central nervous system myelination in human infancy. I. An autopsy study of myelination. *J Neuropathol Exp Neurol* 1987;46(3):283-301
- Holland BA, Haas DK, Norman D, et al. MRI of normal brain maturation. *AJNR* 1986;7:201-208
- Lee BCP, Lipper E, Nass R, et al. MRI of the central nervous system in neonates and young children. *AJNR* 1986;7:605-616
- McArdle CB, Richardson CJ, Nicholas DA, et al. Developmental features of the neonatal brain: MR imaging. Part I. Gray-white matter differentiation and myelination. *Radiology* 1987;162:223-229
- Barkovich AJ, Kjos BO, Jackson DE Jr, et al. Normal maturation of the neonatal and infant brain: MR imaging at 1.5T. *Radiology* 1988;166:173-180
- Curnes JT, Whaley RA, Scatliff JH. Normal brain iron appearance at 0.5 Tesla. Presented at the annual meeting of the American Society of Neuroradiology, New York City, 1987
- Blinkov SM, Glezer II. *The human brain in figures and tables; a quantitative handbook*. New York: Plenum, 1968
- Tomasch J. A quantitative analysis of the human anterior commissure. *Acta Anat (Basel)* 1957;30:902-906
- Naidich TP, Daniels DL, Peck P, et al. Anterior commissure: anatomic-MR correlation and use as a landmark in three orthogonal planes. *Radiology* 1986;158:421-429
- Atlas SW, Zimmerman RA, Bilaniuk LT, et al. Corpus callosum and limbic system: neuroanatomic MR evaluation of developmental anomalies. *Radiology* 1986;160:355-362